Research Article

Meng Song*, Xiulin Yue, Xiujuan Wang, Mengjie Huang, Mingxing Ma, Wei Pan, and Qi Qin*

Improved high-temperature damping performance of nitrile-butadiene rubber/phenolic resin composites by introducing different hindered amine molecules

https://doi.org/10.1515/epoly-2020-0054
received July 04, 2020; accepted August 06, 2020

Abstract: By introducing hindered amine GW-622 or GW-944 into nitrile-butadiene rubber/phenolic resin (NBR/PR, abbreviated as NBPR) matrix, we have prepared different hindered amine/NBR/PR ternary hybrid damping materials with high-temperature damping performance, respectively. Fourier transform infrared (FTIR) spectroscopy, scanning electron microscope (SEM), differential scanning calorimetry (DSC), and dynamic thermomechanical analysis (DMA) were used to research the microstructure, compatibility, and damping properties of the hindered amine/NBPR composites. FTIR results indicate that hydrogen bonds are formed between the hindered amine and the NBPR matrix. Both DSC and SEM results show that hindered amine has partial compatibility with the NBPR matrix. DMA results show that two loss peaks appear in the hindered amine/NBPR composite. Thereby, the composites show better damping performance at a higher temperature, and the temperature domain of high-temperature damping becomes wider with the increase in the addition of hindered amine. This study provides a theoretical support for the preparation of high-temperature damping materials.

Keywords: damping properties, hindered amines, nitrile-butadiene rubber/phenolic resin, ternary hybrid

* **Corresponding author: Meng Song,** School of Materials and Chemical Engineering, Zhongyuan University of Technology, Zhengzhou, 450007, China, e-mail: chengsimengyin@126.com
* **Corresponding author: Qi Qin,** School of Materials and Chemical Engineering, Zhongyuan University of Technology, Zhengzhou, 450007, China, e-mail: qq@zut.edu.cn
Xiulin Yue, Mengjie Huang, Mingxing Ma, Wei Pan: School of Materials and Chemical Engineering, Zhongyuan University of Technology, Zhengzhou, 450007, China
Xiujuan Wang: Key Laboratory of Rubber-plastics, Ministry of Education/Shandong Provincial Key Laboratory of Rubber-plastics, Qingdao University of Science and Technology, Qingdao, China

1 Introduction

Rubber is the most important damping material because of its unique viscoelastic properties (1,2). The damping principle of rubber damping material is to use the viscoelastic property of the polymer to absorb vibration energy (3). The absorbed mechanical energy or sound energy is partially converted into heat energy and dissipated to reduce vibration or reduce amplitude (4). Generally speaking, the damping factor of pure rubber matrix is small, the glass transition temperature (T_g) range is narrow, and the effective damping temperature range is in the low-temperature region below room temperature (5–7). Therefore, the material needs to be modified to achieve the required damping purpose. In recent years, the study of organic hybrid damping materials has attracted much attention (8,9). The damping property of the rubber matrix is improved by hydrogen bond (H-bond) interaction between rubber matrix and polar organic molecules (10).

To prepare organic hybrid materials, hindered phenols containing polar hydroxyl groups are often selected as polar small molecules, such as AO-80 (11), AO-60 (12), and AO-70 (13). Most of the previous studies have been on the binary hybrid damping materials (14,15). At the very beginning, Wu et al. studied the hybrid composites of AO-80/chlorinated polyethylene (CPE) (16), AO-70/CPE and AO-60/CPE (17), and found that the addition of hindered phenol could significantly increase the damping performance of CPE matrix. Zhao et al. added the hindered phenol to the polar nitrile rubber (nitrile butadiene rubber [NBR]) matrix to prepare the rubber-based damping material with high loss peak and improved tensile properties (18). Like hindered phenols, hindered amine molecules contain a large number of polar amine and imine groups. When the hindered amine is added to the polar rubber, it can interact with the polar rubber matrix, thus giving the rubber matrix excellent damping properties (19). Besides, the hindered amine has wide sources and is of lower price than hindered phenol, which can effectively reduce the production cost of organic

hybrid materials. Therefore, it is of great significance to study hindered amine/rubber composites.

The damping properties of binary rubber-based organic hybrid materials tend to be improved at room temperature (20,21). However, the processing and use environment of rubber damping materials is changeable, so it is of great significance to prepare materials with high damping properties in a wide temperature range, especially in a high-temperature range. Researchers began to prepare ternary hybrid damping materials by adding polar small molecules to rubber and plastic blends. Zhang et al. prepared hindered phenol AO-80/phenol resin (PR)/NBR ternary hybrid with long-period damping properties (22). In our previous study, by introducing AO-80 into nitrile butadiene rubber/poly(vinyl chloride) (NBR/PVC), we got ternary hybrid damping materials with high damping properties and high mechanical properties (23).

In this study, we propose a strategy that many hydroxyl polar functional groups in the phenolic resin structure, which would lead to a polar amino group on the hindered amine, can form strong H-bond with NBR and PR matrix to prepare high damping materials in the high-temperature domain. Nitrile butadiene rubber/phenolic resin (NBR/PR [NBPR]) was selected as matrix, and different kinds of hindered amines (GW-622 and GW-944) were chosen as polar small molecules to prepare ternary hybrid damping materials. NBR exhibits excellent damping performance due to the presence of polar cyan functional groups in its structure.

2 Experimental

2.1 Materials

Hindered amine powders (GW-622 and GW-944) were supplied by Beijing Additives Institute (China). NBR with an acrylonitrile weight content of 41% (N220S) was provided by Japan Synthetic Rubber Co., Ltd (Japan). Phenolic resin powders (PR 2123) were obtained from Wuxi Mingyang Bonding Material Co., Ltd (China). Other rubber processing additives were of analytical grade and used without further purification. The chemical structures of GW-622 and GW-944 are shown in Figure 1.

2.2 Preparation of hindered amine/NBPR composites

The NBPR composites were obtained by mixing the NBR and PR powders (the mass ratio of NBR and PR is 80:20) in φ152.4 mm two-roll mill at room temperature. The mixture was then added with different masses of hindered amine molecules, and the mass ratios of GW-622 and NBPR were 0/100, 17/100, 35/100, 52/100, and 70/100 (the mass ratios of GW-944 and NBPR were 0/100, 18/100, 36/100, 54/100, and 72/100). The mixtures were then kneaded at 130°C for 5 min on a two-roll mill to fully fuse the hindered amine molecules.

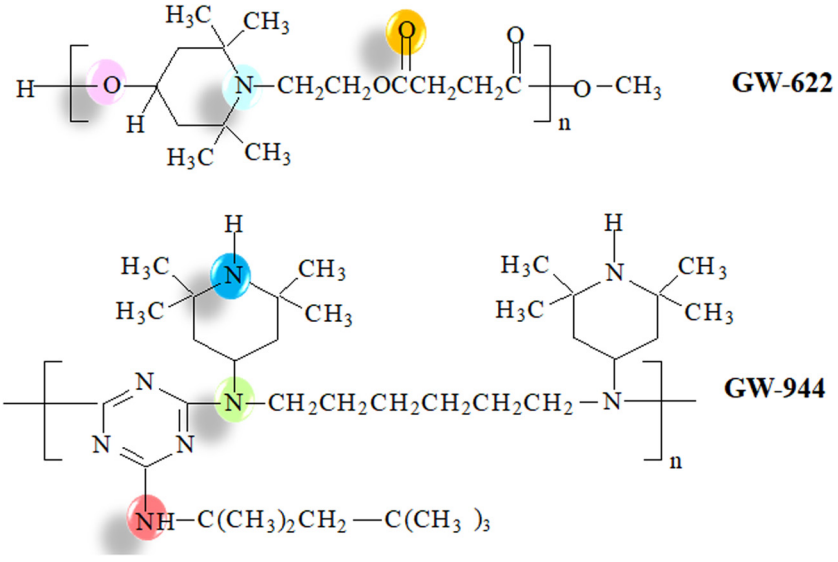

Figure 1: Chemical structures of GW-622 and GW-944 molecules.

Then, the compounding and crosslinking additives were added to the above mixtures, including 5.0 phr of zinc oxide, 2.0 phr of stearic acid, 0.2 phr of tetramethylthiuram disulfide, 0.5 phr of diphenyl guanidine, 0.5 phr of dibenzothiazole disulfide, and 2.0 phr of sulfur. Finally, the mixtures were hot pressed and vulcanized at 160°C and 15 MPa for their corresponding T90 (optimum cure time).

2.3 Characterization

Fourier transform infrared spectroscopy (FTIR) was conducted by Nicolet 8700, Thermo Fisher Scientific Inc. (USA). The spectra were obtained by using the attenuated total reflection technique in a wavenumber ranging from 4,000 cm^{-1} to 500 cm^{-1} for 32 scans at a resolution of 8 cm^{-1}. The GW-622 (or GW-944) powder spectra were obtained by using ultrathin disk specimens pressed from hindered amine ground in anhydrous potassium bromide.

Scanning electron microscopy (SEM) images of the fracture surfaces of the hindered amine/NBPR composites were taken by Hitachi S-4800 (Japan). All SEM samples were cryogenically fractured by quenching in liquid nitrogen.

Differential scanning calorimetry (DSC) was performed on a TGA/DSC calorimeter, Mettler-Toledo Co (Switzerland). Samples were heated from −60°C to 150°C at a heating rate of 20°C/min under an N_2 atmosphere.

Dynamic mechanical performance (dynamic thermomechanical analysis [DMA]) was attained by VA 3000 dynamic mechanical analyzer, Rheometric Scientific Inc. (USA). The sample size was 15 mm (length) × 10 mm (width) × 2 mm (thickness). The temperature range was

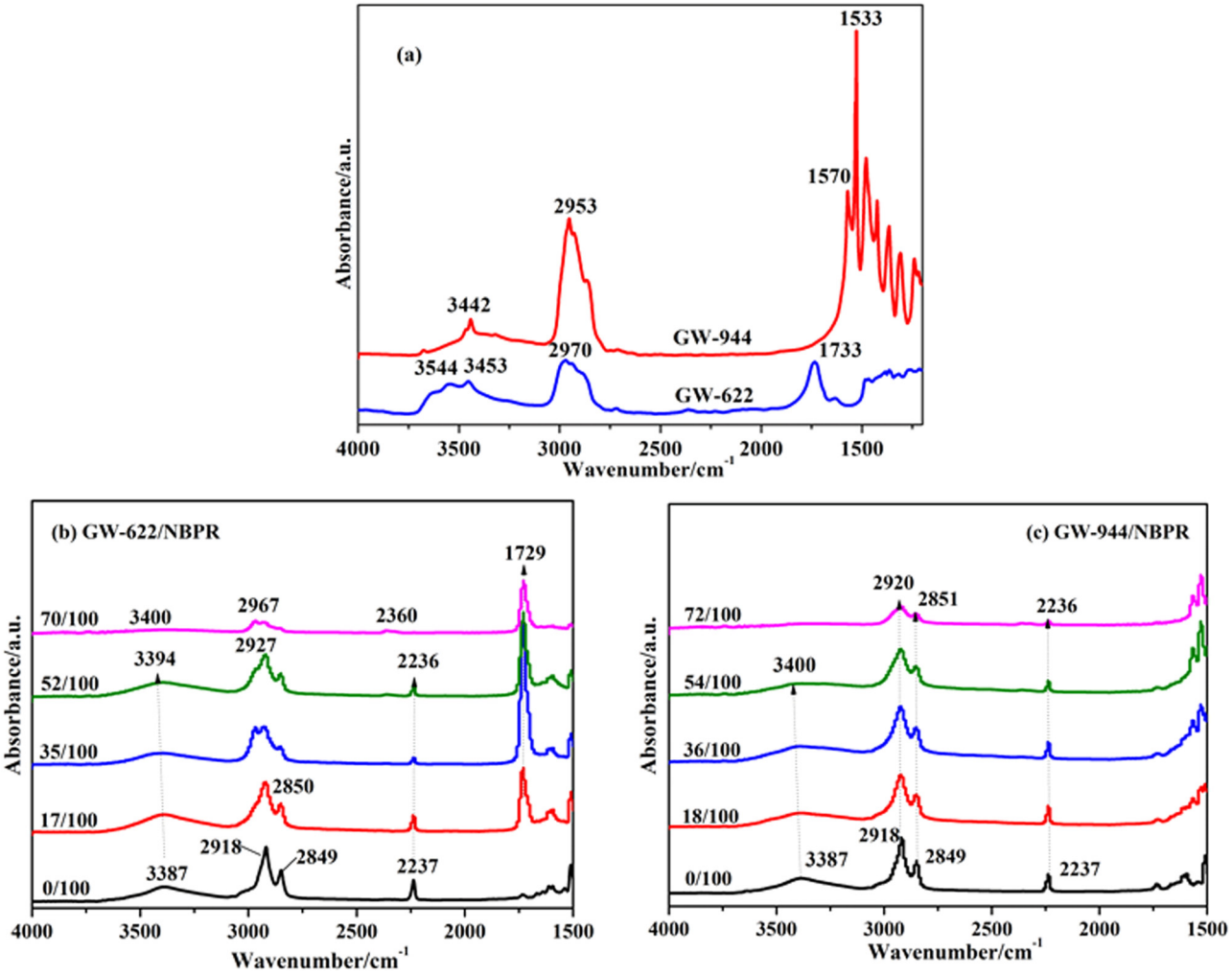

Figure 2: FTIR spectra of (a) GW-622 and GW-944 molecule, (b) GW-622/NBPR composites, and (c) GW-944/NBPR composites.

measured form −100°C to 200°C at a heating rate of 5°C/min and a constant frequency of 10 Hz.

3 Results and discussion

3.1 Hydrogen bonding interactions of hindered amine/NBPR composites

To test our prepared samples, the classical FTIR measurements were used to detect the intermolecular interactions between the hindered amine molecules and NBPR matrix, as shown in Figure 2. Two prominent absorption peaks appear at 3,544 and 3,453 cm^{-1} in Figure 2a, corresponding to the free hydroxyls of GW-622 molecules and the H-bond interactions (O–H···O H-bonds) between GW-622 molecules (19). The peak at 1,733 cm^{-1} wavenumber is attributed to the carbonyl groups. For GW-944 molecules, the peak at the wavenumber 3,442 cm^{-1} belongs to the amino groups. Figure 2b shows that pure NBPR matrix has two distinct peaks. The broad infrared absorption peak in the wavenumber ranging from 3,250 to 3,500 cm^{-1} is responsible for phenolic hydroxyl groups of PR (22). The –CN group of NBR is at wavenumber 2,237 cm^{-1} (23). With the increasing addition of GW-622 molecules, it can be found that the 3,387 peak intensity decrease and the peak shifts to the high wavenumber, which means more phenolic hydroxyl groups involves in the formation of H-bonds. Similarly, the –CN groups also change accordingly, indicating that more –CN groups are involved in the formation of H-bonds.

Figure 2c shows that the addition of hindered amine GW-944 into NBPR matrix has a similar effect as GW-622. With increasing the content of GW-944 molecules, the 2,237 cm^{-1} peak of –CN groups decreases gradually. Also, the vibration peak of phenolic hydroxyl group moves toward high wavenumber, and the phenomenon of blue shift occurs. These phenomena indicate that the addition of GW-944 molecules increase the content of intermolecular H-bonds in the NBPR composites.

3.2 Microstructure of hindered amine/NBRR composites

To illustrate the microstructure morphology of hindered amine/NBPR composites, the SEM test is carried out, as shown in Figure 3. Figure 3a and b shows that pure NBPR

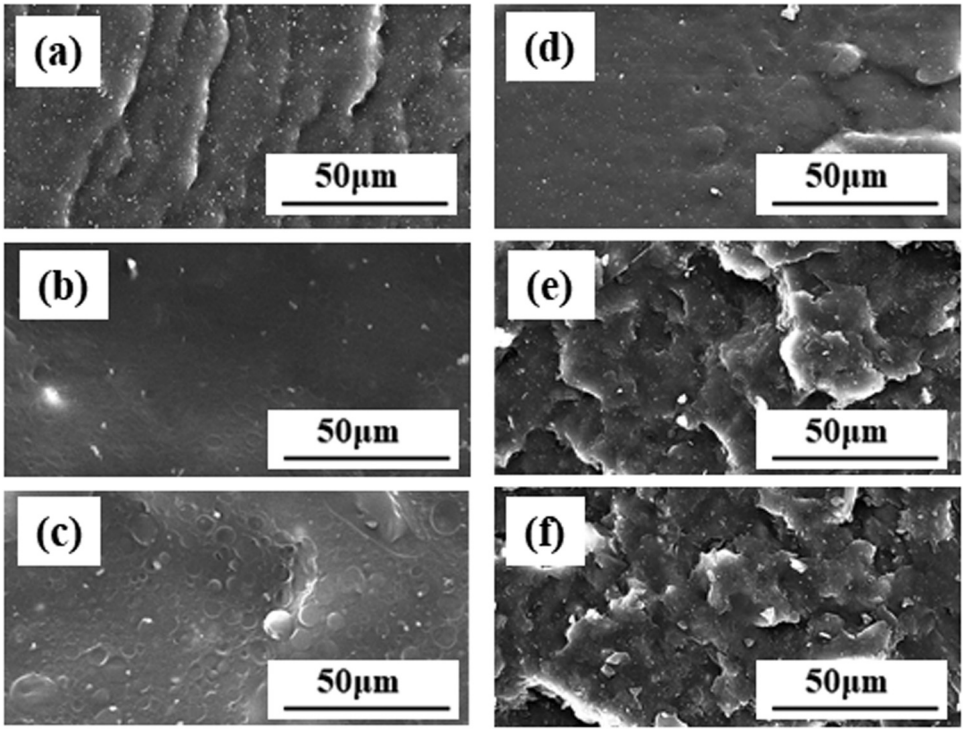

Figure 3: SEM images of NBPR composites filed with (a) 0 phr, (b) 35 phr, and (c) 52 phr GW-622, and SEM images of NBPR composites filed (d) 0 phr, (e) 36 phr, and (f) 54 phr GW-944.

samples have smooth fracture surfaces, indicating the good compatibility between the NBR and PR. When the content of GW-622 is above 35 phr, some pits begin to protrude on the surface of GW-622/NBPR composite, as shown in Figure 3c and d. The dispersion of small molecules in the NBPR has reached a saturation state. The addition of more GW-622 will cause the aggregation of small molecules. During the embrittlement and cold breaking in liquid nitrogen, the aggregates of GW-622 molecules fell off from the surface of the NBPR matrix, resulting in the formation of pits. At the same time, the partial compatibility between GW-622 molecules and the NBPR matrix is also the cause of the uneven surface.

On the basis of the microstructure morphology test, we could clearly compare with our prepared samples with GW-622/NBPR composites, and the GW-944/NBPR composites become rougher when the addition of GW-944 small molecules reaches 36 phr. This may be due to the uneven size of the hindered amine GW-944, ranging from micron to millimeter, and so it is difficult for GW-944 to be uniformly dispersed in the NBPR matrix.

3.3 Glass transition of hindered amine/NBPR composites

Further analysis of the thermal stability of the prepared sample was carried out, and Figure 4 shows the DSC curves of the hindered amines molecules and the hindered amine/NBPR composites with different mass ratios. As shown in Figure 4a, the glass transition temperatures of hindered amine GW-622 and GW-944 are 67.6°C and 84.8°C, respectively. As shown in Figure 4b, T_g of NBPR matrix is 0.1°C, and the melting temperature of NBPR is 109.2°C. Figure 4b shows that T_g of GW-622/NBPR composite moves toward low temperature in a small extent with the addition of GW-622 molecules. With the formation of the molecular interaction between GW-622 and NBPR, theoretically, T_g should move toward high temperature. However, due to the large molecular structure of GW-622 (as shown in Figure 1), the volume of GW-622/NBPR composites becomes larger when there is an increase in the addition of GW-622, making T_g move toward the low temperature.

Similar results were observed for the GW-944/NBPR composite, i.e., adding GW-622 molecules and making T_g to move toward the low temperature. We will further verify the aforementioned results.

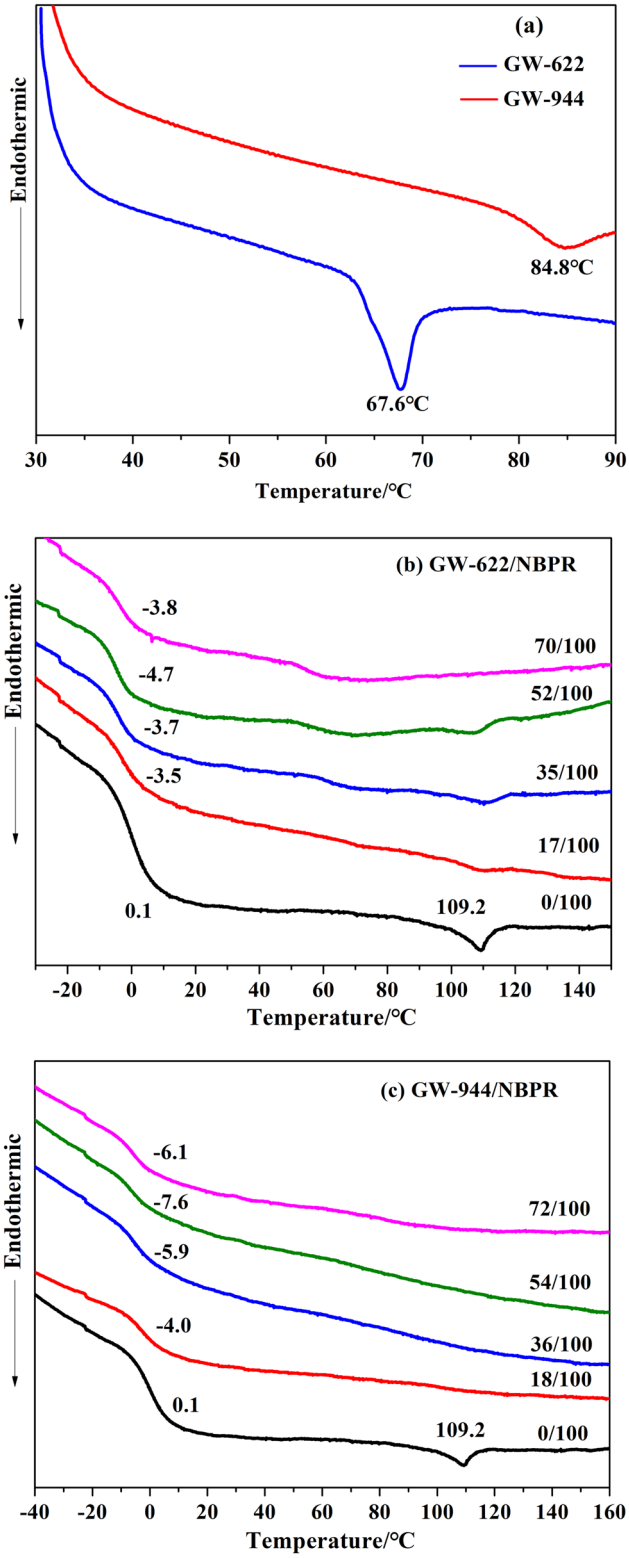

Figure 4: DSC curves of (a) GW-622 and GW-944 molecule, (b) GW-622/NBPR composites, and (c) GW-944/NBPR composites.

3.4 Damping properties of hindered amine/NBPR composites

The damping properties of materials are determined by the loss factor and the area of the glass transition zone (TA value) ($\tan\delta > 0.3$) (24,25). Figure 5 shows the temperature dependence of the $\tan\delta$ value of hindered amine/NBPR composite. The pure NBPR matrix has only one loss peak, which again indicates the good compatibility between NBR and PR, as shown in the earlier SEM. As shown in Figure 5a, with the addition of GW-622 molecules, the GW-622/NBPR composites change from a single loss peak to two adjacent double loss peaks. Moreover, with the increasing GW-622 contents, the first loss peak in the room temperature region decreases and moves toward the low-temperature direction, as shown in the aforementioned DSC. The second loss peak in the high-temperature region increases gradually, and the range of damping temperature domain also increases gradually with the addition of GW-622 molecules. From Table 1, we can observe that the first loss peak value of GW-622/NBPR decreases from the original 1.28 to 0.87 by 32%. The TA_1 value also has a 43.6% decrement from 38.61 to 21.78. The peak position moves from 29.88 to 23.14, which is consistent with the aforementioned DSC analysis. The second loss peak value increases from the original 0.20 to 0.64 by 220%. In addition, the TA_2 value has a greater increment from 6.52 to 27.79.

Figure 5b shows that the addition of GW-944 molecules also makes the GW-944/NBPR composite show two loss peaks. Compared with the addition of GW-622, the addition of GW-944 reduces the first loss

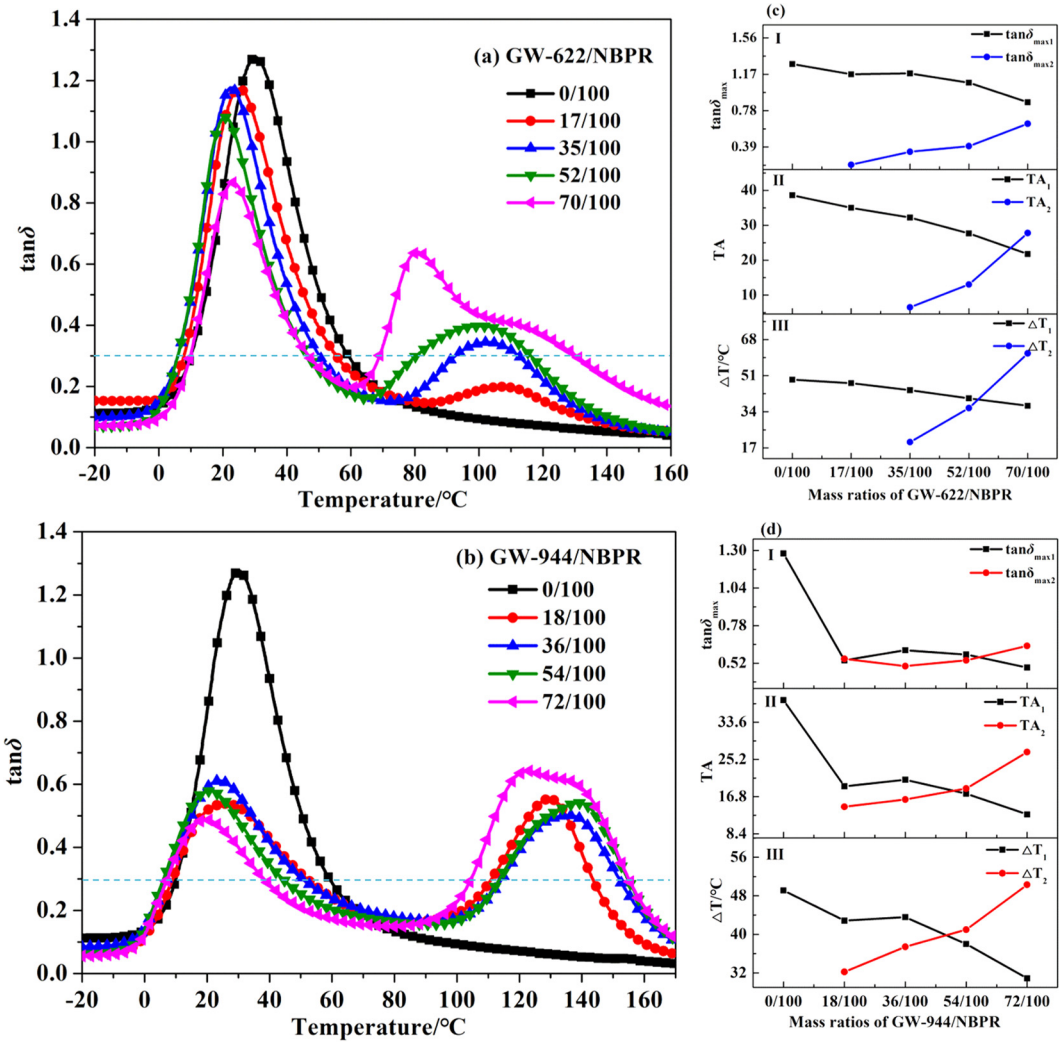

Figure 5: Temperature dependence of tan δ of (a) GW-622/NBPR composites, (b) GW-944/NBPR composites, (c) damping parameter variation of GW-622/NBPR, and (d) damping parameter variation of GW-944/NBPR.

Table 1: Damping properties of the GW-622/NBPR composite with different GW-622 molecule contents

GW-622/NBPR	$T < 50$ (°C)				$T > 50$ (°C)			
	tan δ peak position (°C)	tan δ peak height	Temperature range >0.3		tan δ peak position (°C)	tan δ peak height	Temperature range >0.3	
			ΔT_1 (°C)	TA_1			ΔT_2 (°C)	TA_2
0/100	29.88	1.28	49.12	38.61	—	—	—	—
17/100	25.19	1.17	47.49	35.00	107.34	0.20	—	—
35/100	22.22	1.18	44.14	32.22	102.56	0.34	19.78	6.52
52/100	20.04	1.08	40.35	27.68	99.99	0.40	35.76	13.05
70/100	23.14	0.87	36.82	21.78	80.74	0.64	61.50	27.79

peak of the NBPR matrix more and increases the second loss peak of the matrix more. From Table 2, we can observe that the first loss peak decreases by 61.7% from 1.28 to 0.49, whereas the second loss peak increases from 0.55 to 0.64.

Figure 5c and d shows that the loss factor value of hindered amine/NBPR composites in the low-temperature zone (−80°C to 60°C) decreases with the addition of the hindered amine, while the loss factor value of the composite in the high-temperature zone (80–140°C) increases continuously, indicating that the addition of hindered amine GW-622 or GW-944 can effectively improve the damping performance of the NBPR matrix in the high-temperature zone. When the hindered amine molecules are added to the NBPR matrix, the H-bond interactions formed between hindered amine molecules and the NBPR matrix. At the same time, saturated small molecules are dispersed in the NBPR matrix, the addition of more hindered amines would result in the aggregation in small molecules. As a result, the volume of hindered amine/NBPR composites increases, resulting in T_g of composites moving toward the direction of high temperature and decreasing of the loss factor value in the room temperature.

Figure 6 shows the temperature dependence of storage modulus (E') of hindered amine/NBPR composites. As shown in Figure 6, the higher the content of the hindered amine molecules, the greater the storage modulus of the composites (26). The E' is a measure of the capability of the composites to store mechanical energy and resist deformation (11,27). This is due to the formation of H-bond between hindered amine molecules and the NBPR matrix, which increases the E' of the composites. It is noteworthy that the material has a wide glass transition zone, that is, the addition of small molecules to broaden the application range of damping materials.

4 Conclusions

Herein, by introducing different hindered amine molecules into the NBPR matrix, we prepared different hindered amine/NBPR ternary hybrid damping materials. FTIR, DSC, SEM, and DMA were used to characterize the microstructure, compatibility, and damping performance of the hindered amine/NBPR composites as follows:

1. FTIR results show that H-bonds are formed between the hindered amine and the NBPR matrix.
2. DSC and SEM results indicate that GW-622 has partial compatibility with the NBPR matrix when the addition

Table 2: Damping properties of the GW-944/NBPR composite with different GW-944 molecule contents

GW-944/NBPR	$T < 50$ (°C)				$T > 50$ (°C)			
	tan δ peak position (°C)	tan δ peak height	Temperature range >0.3		tan δ peak position (°C)	tan δ peak height	Temperature range >0.3	
			ΔT_1 (°C)	TA_1			ΔT_2 (°C)	TA_2
0/100	29.88	1.28	49.12	38.61	—	—	—	—
18/100	25.65	0.54	42.85	19.14	129.39	0.55	32.23	14.51
36/100	23.85	0.61	43.57	20.63	136.04	0.50	37.43	16.17
54/100	20.67	0.58	38.01	17.47	139.07	0.54	40.98	18.64
72/100	19.42	0.49	30.88	12.80	122.91	0.64	50.32	26.88

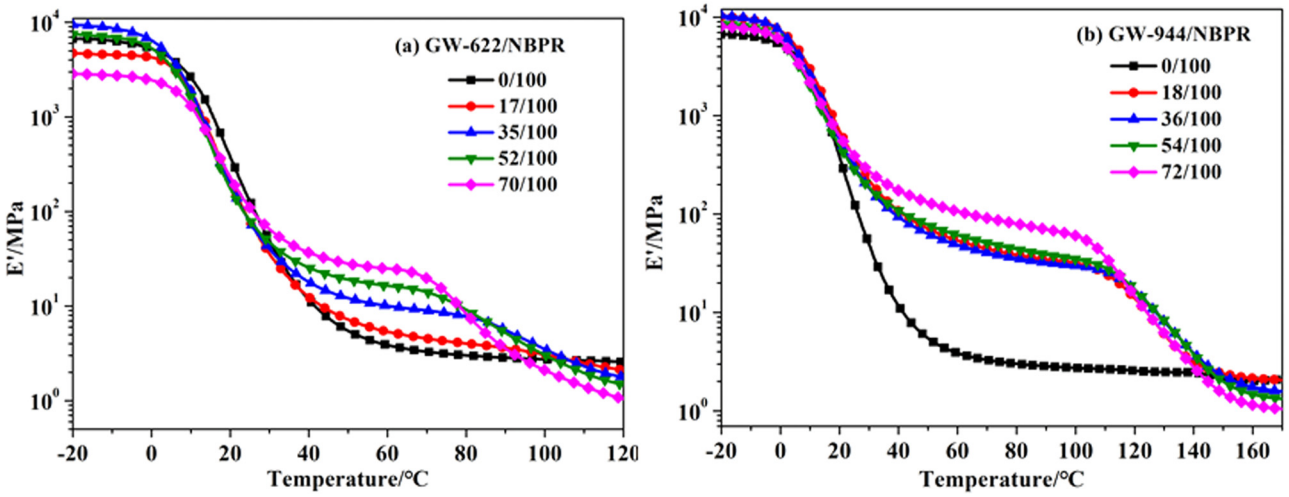

Figure 6: Temperature dependence of storage modulus (E') of (a) GW-622/NBPR composites and (b) GW-944/NBPR composites.

exceeds 35 phr. For GW-944 composites, phase splitting occurs when the addition of GW-944 molecules is more than 36 phr.

3. DMA results show that hindered amine/NBPR composites appear two loss peaks. The first loss peak value decreases, and the second loss peak value increases with the increasing hindered amine contents. The TA_2 value of GW-622/NBPR composite has a greater increment from 6.52 to 27.79, while the TA_2 value of GW-944/NBPR composite increases from 14.51 to 26.88. The high-temperature damping domains of both composites are broadened.

Acknowledgments: This work was supported by the National Natural Science Foundation of China under Grant (No. 51603236, 51703114); the Program for Henan Science and Technology Department of Science and Technology Research (No. 172102210073); the Program for Interdisciplinary Direction Team in Zhongyuan University of Technology, China; Key Scientific Research Project Plan of Henan University (No. 20B430022); and the Independent Innovation Application Research Project of Zhongyuan University of Technology (No. K2018YY029).

Conflict of interest: The authors declare no competing financial interest.

References

(1) Xiao DL, Zhao XY, Feng Y, Xiang P, Zhang LQ. The structure and dynamic properties of thermoplastic polyurethane elastomer/hindered phenol hybrids. J Appl Polym Sci. 2010;4(116):2143–50.

(2) Xu KM, Hu QM, Wu H, Guo SY, Zhang FS. Designing a polymer-based hybrid with simultaneously improved mechanical and damping properties via a multilayer structure construction: structure evolution and a damping mechanism. Polymers. 2020;2(12):446.

(3) Song M, Zhao XY, Li Y, Hu SK, Zhang LQ, Wu SZ. Molecular dynamics simulations and microscopic analysis of the damping performance of hindered phenol AO-60/nitrile-butadiene rubber composites. RSC Adv. 2014;4(13):6719–29.

(4) Zhao XY, Cao YJ, Zou H, Li J, Zhang LQ. Structure and dynamic properties of nitrile-butadiene rubber/hindered phenol composites. J Appl Polym Sci. 2012;6(123):3696–702.

(5) Shi GP, Yin XT, Wu GZ. Thermodynamic phase analysis of acrylic polymer/hindered phenol hybrids: effects of hydrogen bonding strength. Polymer. 2018;153:317–24.

(6) Zhu J, Zhao XY, Liu L, Song M, Wu SZ. Quantitative relationships between intermolecular interaction and damping parameters of irganox-1035/NBR hybrids: acombination of experiments, molecular dynamics simulations, and linear regression analyses. J Appl Polym Sci. 2018;17(135):46202.

(7) Zhang JH, Wang LF, Zhao YF. Fabrication of novel hindered phenol/phenol resin/nitrile butadiene rubber hybrids and their long-period damping properties. Polym Composite. 2012;12(33):2125–33.

(8) Zhang L, Chen DL, Fan XQ, Cai ZB, Zhu MH. Effect of hindered phenol crystallization on properties of organic hybrid damping materials. Materials. 2019;7(12):1008.

(9) Yin XT, Liu CY, Lin Y, Guan AG, Wu GZ. Influence of hydrogen bonding interaction on the damping properties of poly(*n*-butyl methacrylate)/small molecule hybrids. J Appl Polym Sci. 2015;19(132):41954.

(10) Xu KM, Hu QM, Wang JH, Zhou HD, Chen JL. Towards a stable and high-performance hindered phenol/polymer-based damping material through structure optimization and damping mechanism revelation. Polymers. 2019;5(11):884.

(11) Qiao B, Zhao XY, Yue DM, Zhang LQ, Wu SZ. A combined experiment and molecular dynamics simulation study of

hydrogen bonds and free volume in nitrile-butadiene rubber/hindered phenol damping mixtures. J Mater Chem. 2012;22:12339–48.
(12) Song M, Zhao XY, Li Y, Chan TW, Zhang LQ, Wu SZ. Effect of acrylonitrile content on compatibility and damping properties of hindered phenol AO-60/nitrile-butadiene rubber composites: molecular dynamics simulation. RSC Adv. 2014;4(89):48472–9.
(13) Xu KM, Zhang FS, Zhang XL, Hu QM, Wu H, Guo SY. Molecular insights into hydrogen bonds in polyurethane/hindered phenol hybrids: evolution and relationship with damping properties. J Mater Chem A. 2015;2(22):8545–56.
(14) Yin C, Zhao XY, Zhu J, Hu HH, Song M, Wu SZ. Experimental and molecular dynamics simulation study on the damping mechanism of C5 petroleum resin/chlorinated butyl rubber composites. J Mater Sci. 2019;54:3960–74.
(15) Li MJ, Zhu WH, Xu YW, Fu MS, Cao YH. Preparation and damping properties of (waste rubber powder)/hindered phenol composites. J Vinyl Addit Techn. 2014;4(20):225–9.
(16) Wu CF, Yamagishi TA, Nakamoto Y, Ishida SI, Nitta KH. Organic hybrid of chlorinated polyethylene and hindered phenol. I. Dynamic mechanical properties. J Polym Sci Pol Phys. 2000;17(38):2285–95.
(17) Wu CF, Yamagishi TA, Nakamoto Y, Ishida SI, Kubota S, Nitta KH. Organic hybrid of chlorinated polyethylene and hindered phenol. II. Influence of the chemical structure of small molecules on viscoelastic properties. J Polym Sci Pol Phys. 2000;11(38):1496–503.
(18) Zhao XY, Xiang P, Tian M, Fong H, Jin R, Zhang LQ. Nitrile butadiene rubber/hindered phenol nanocomposites with improved strength and high damping performance. Polymer. 2007;20(48):6056–63.
(19) Song M, Wang XJ, Wu SZ, Qin Q, Yu GM, Liu ZZ, et al. How the hindered amines affect the microstructure and mechanical properties of nitrile-butadiene rubber composites. e-Polymers. 2020;1(20):8–15.
(20) Wu CF, Mori K, Otani Y, Namiki N, Emi H. Effects of molecule aggregation state on dynamic mechanical properties of chlorinated polyethylene/hindered phenol blends. Polymer. 2001;19(42):8289–95.
(21) Zhu J, Zhao XY, Liu L, Yang RN, Song M, Wu SZ. Thermodynamic analyses of the hydrogen bond dissociation reaction andtheir effects on damping and compatibility capacities of polar smallmolecule/nitrile-butadiene rubber systems: molecular simulation andexperimental study. Polymer. 2018;155:152–67.
(22) Zhang JH, Wang LF, Zhao YF. Fabrication of novel hindered phenol/phenol resin/nitrile butadiene rubber hybrids and their long-period damping properties. Polym Compos. 2012;33(12):2125–33.
(23) Song M, Zhao XY, Chan TW, Zhang LQ, Wu SZ. Microstructure and dynamic properties analyses of hindered phenol AO-80/nitrile-butadiene rubber/poly (vinyl chloride): a molecular simulation and experimental study. Macromol Theory Simul. 2015;1(24):41–51.
(24) Xu KM, Zhou HD, Hu QM, Wang JH, Huang Y, Chen JL. Molecular insights into chain length effects of hindered phenol on the molecular interactions and damping properties of polymer-based hybrid materials. Polym Eng Sci. 2020;3(60):446–54.
(25) Zhao XY, Zhang G, Lu F, Zhang LQ, Wu SZ. Molecular-level insight of hindered phenol AO-70/nitrile-butadiene rubber damping composites through a combination of a molecular dynamics simulation and experimental method. RSC Adv. 2016;6(89):85994–6005.
(26) Hilmi AR, Fauziyah NA, Pratapa S. A temperature-dependent storage modulus model for filler-dispersed PEG/silica composites. Composites Part B. 2019;173:079.
(27) Laurent C, Simon J. Modelling the storage modulus, transition temperatures and time–temperature superposition characteristics of epoxies and their composites. J Therm Anal Calorim. 2018;3(131):2589–601.